

Dear editor and reviewers,

We appreciate your arduous work and constructive comments. We have revised the manuscript carefully according to the comments.

## **Reviewer #1**

Ocean color observations are demonstrated to be useful in investigating small-scale processes in the South China Sea. It is true that conventional satellite observations, such as altimetry products may not resolve such proposes with adequate spatial resolutions (along-track data may have high resolutions, but merged grid data generally have low resolutions). In contrast, the high-resolution ocean color data products have their advantages. The authors provide a good example by examining the propagation process of small-scale cyclonic eddies in the western South China Sea. They also try to make a perspective explanation about the underlying physical processes that influence the formation of the small-scale eddies. Overall, I think it is a good contribution to the marine remote sensing and applied oceanography community. The paper is also concise and easy to read. I would suggest it be accepted for publication after some minor revisions in both text and figures.

Specific comments listed as follows:

P13516, L5, “the order of” can be removed from the sentence.

[Reply: We have removed "the order of" in the revised manuscript.](#)

P13519, L12, “NOAA” should be mentioned here.

[Reply: We have added " National Oceanic and Atmospheric Administration \(NOAA\)" here and also added it in the acknowledgements sections.](#)

P13519, L15-17, the sentence should be rewritten: “where tauy is the wind stress parallel to the coastline, positive northward. It is replaced with the meridional direction wind stress since the most significant offshore transport perpendicular to the Vietnam coast is approximately in the zonal direction.”

[Reply: Thanks a lot. We have rewritten the sentence.](#)

P13522, L1, “to” should be removed from the sentence.

[Reply: We have removed "to" in this sentence.](#)

P13522, L14, “tends” should be changed to “tend”.

[Reply: We have changed "tends" to "tend". Thanks a lot.](#)

Figure 3, better use the same lat and lon limits for the three panels on the right (Figures 3b, 3d, 3f). Currently, the high chlorophyll plume in Figure 3f appears to have much larger size than those in Figures 3b & 3d, which may not be true.

Reply: We checked the figure 3, and found that we used the same lat and lon limits for figures 3b, 3d, 3f. The mistake is that we plotted the inconsistent red boxes in figures 3c and 3e in the initial manuscript. We have redrawn the figure 3 in the revised manuscript. It is shown that there is a significant phytoplankton increase in figure 3f. This may be due to a lag between nutrients input and phytoplankton growth.

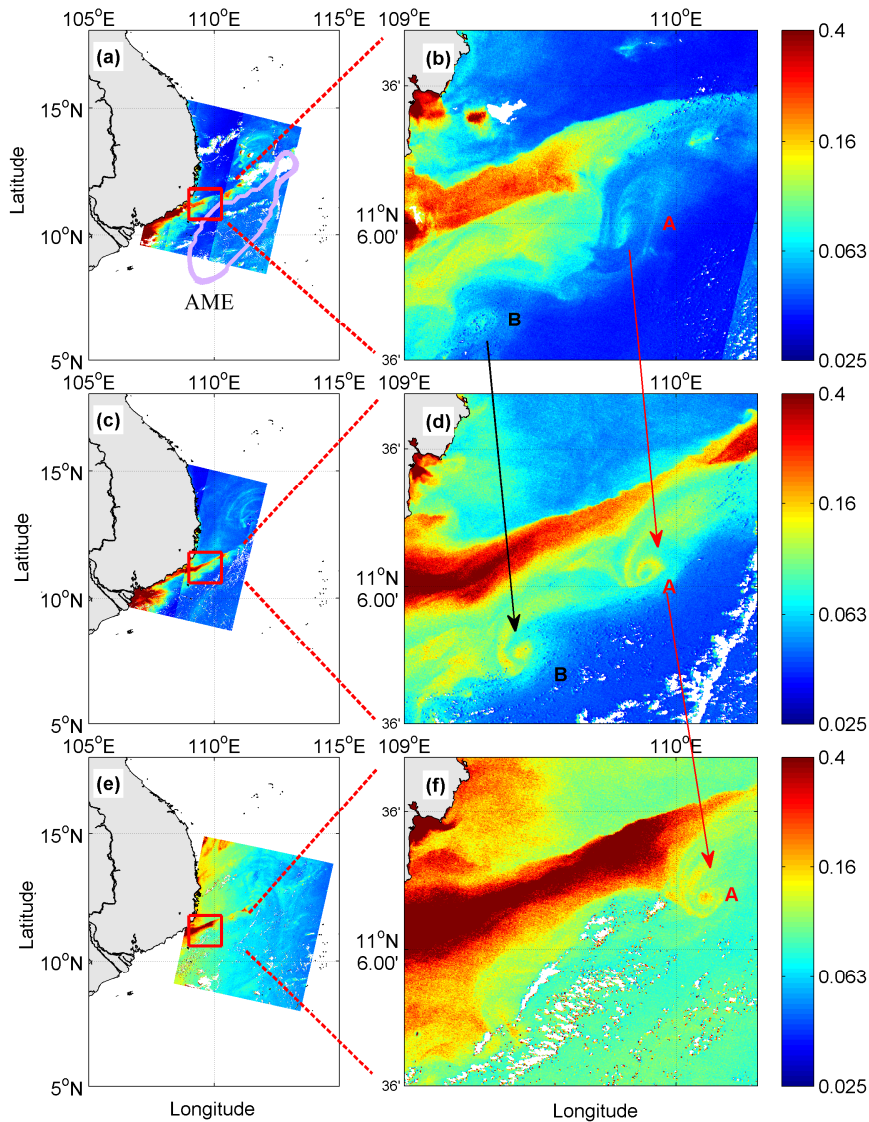


Figure 3. Daily 300 m MERIS chlorophyll (unit:  $\text{mg m}^{-3}$ ) on (a) 9 July 2008, (b) 12 July 2008, (c) 13 July 2008. The cloud covered area is masked by the white color. 'A' and 'B' indicate two small cyclonic eddies respectively. The pink circle in (a) denotes the anticyclonic mesoscale eddy (AME) on 9 July 2008, which is derived from AVISO MSLA data following the method of Chelton et al. (2011).

Figure 5, it is not clear which mesoscale anticyclonic eddy is referred to in the figure caption. Better to specify it in Figures 2 and/or 3.

Reply: We have specified the anticyclonic mesoscale eddy (AME) in Figure 3(a) (shown above).

Thank you again for reviewing our manuscript.

## **Reviewer #2**

This is a short paper that describes some small eddies along an upwelling front in the South China Sea. There are a few speculations about mechanisms, but nothing definitive.

Reply: The physical mechanisms responsible for the genesis of the small-scale eddies are complicated. Researchers accounted for the genesis of the small-scale eddy for some reasons, such as topography, wind, upwelling, mesoscale eddy, but there is still much that is not known. The temporal evolution (of the order of days) and spatial scale (less than 50 km) of the small-scale eddy require adequately resolved time series and the spatial resolution. The present ocean dynamic satellite has limitations in observation of small-scale eddies because of the coarse resolution. So, we have difficulty to get a definitive mechanism based on the present satellite observation.

Starting on page 13521, line 5, there is an attempt to relate these small eddies to some mesoscale feature. I do not understand the approach. I believe that an extra figure showing the mesoscale and submesoscale eddies would be helpful here.

Reply: We have specified the anticyclonic mesoscale eddy (AME) in Figure 3(a). Figure 3 shows the anticyclonic mesoscale eddy (AME), small-scale phytoplankton tendrils and the offshore phytoplankton filaments (shown below). The small-scale eddies along the front of the filament are associated with the occurrence of a mesoscale anticyclonic eddy. The generation of the small-scale eddies may be related to the interaction of the offshore current and the mesoscale anticyclonic eddy. Based on it, we tried to find the relationship of the small-scale eddy with the relative movement of the offshore current and the mesoscale anticyclonic eddy.

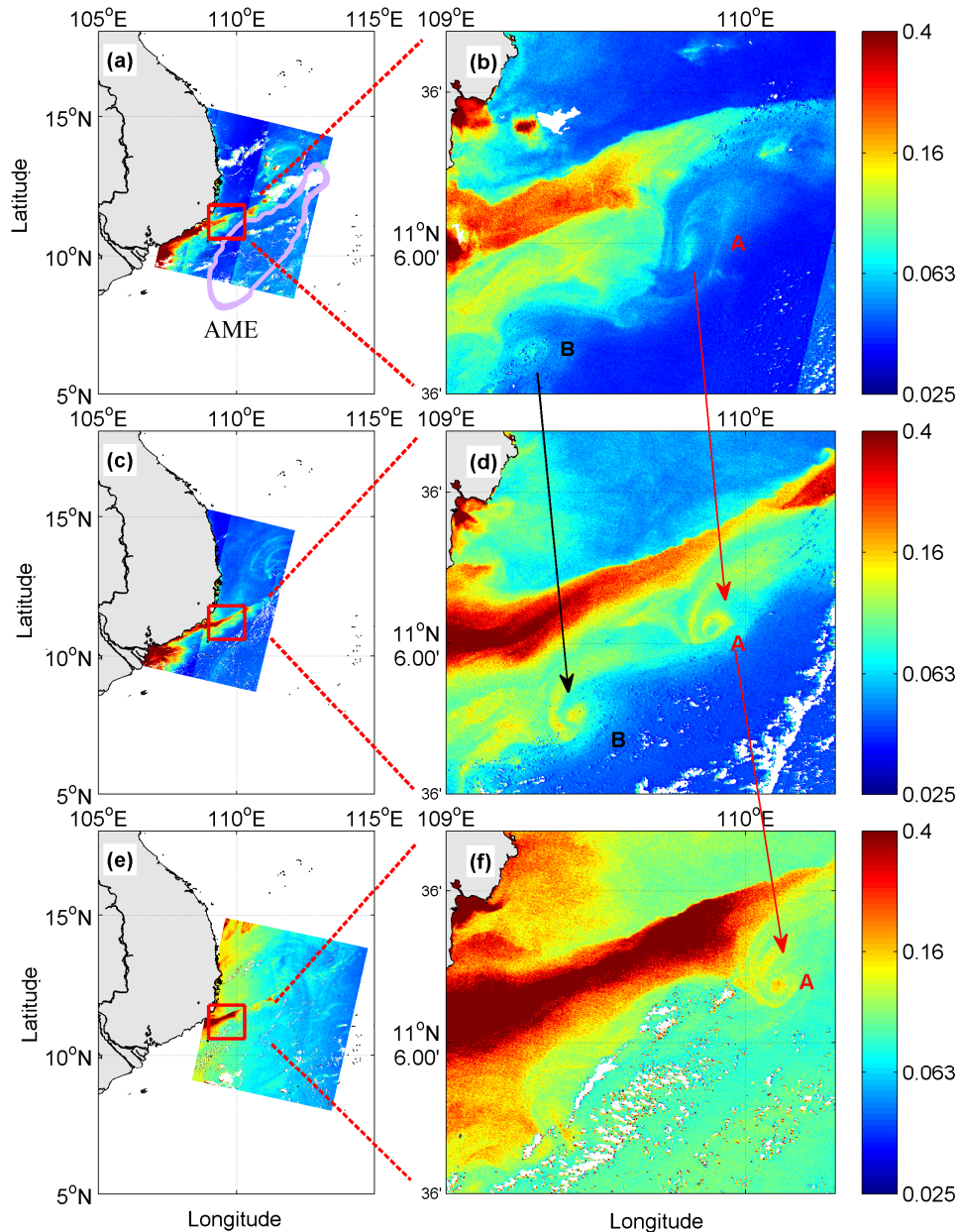


Figure 3. Daily 300 m MERIS chlorophyll (unit:  $\text{mg m}^{-3}$ ) on (a) 9 July 2008, (b) 12 July 2008, (c) 13 July 2008. The cloud covered area is masked by the white color. ‘A’ and ‘B’ indicate two small cyclonic eddies respectively. The pink circle in (a) denotes the anticyclonic mesoscale eddy (AME) on 9 July 2008, which is derived from AVISO MSLA data following the method of Chelton et al. (2011).

This paper is harmless, describes some interesting features and so is publishable after some revisions.

Thank you again for reviewing our manuscript.

1  
2  
3  
4  
5  
6  
7  
8  
9  
10  
11  
12  
13  
14  
15  
16  
17  
18

Satellite observations of the small-scale cyclonic eddies in the western  
South China Sea

Fenfen Liu<sup>1</sup>, Shilin Tang<sup>2,\*</sup>, and Chuqun Chen<sup>2</sup>

<sup>1</sup> School of Marine Sciences, Sun Yat-sen University, [Guangzhou 510006, China](#)

<sup>2</sup> State Key Laboratory of Tropical Oceanography, South China Sea Institute of Oceanology, Chinese Academy of Sciences, Guangzhou 510301, China

\* Corresponding author: Shilin Tang, State Key Laboratory of Tropical Oceanography, South China Sea Institute of Oceanology, Chinese Academy of Sciences, Guangzhou 510301, China. (sltang2009@gmail.com)

19

## 20 **Abstract**

21 High-resolution ocean color observation offers an opportunity to investigate the  
22 oceanic small-scale processes. In this study, The Medium Resolution Imaging  
23 Spectrometer (MERIS) daily 300-m data are used to study small-scale processes in  
24 the western South China Sea. It is indicated that the cyclonic eddies with horizontal  
25 scales of ~~the order of~~ 10 km are frequently observed during upwelling season of each  
26 year over 2004-2009. These small-scale eddies are generated in the vicinity of the  
27 southern front of the cold tongue, and then propagate eastward with a speed of  
28 approximately  $12 \text{ cm s}^{-1}$ . This propagation speed is consistent with the velocity of the  
29 western boundary current. As a result, the small-scale eddies keep rotating high levels  
30 of the phytoplankton away from the coastal areas, resulting in the accumulation of  
31 phytoplankton in the interior of the eddies. The generation of the small-scale eddies  
32 may be associated with strengthening of the relative movement between the rotation  
33 speed of the anticyclonic mesoscale eddies and the offshore transport. With the  
34 increases of the normalized rotation speed of the anticyclonic mesoscale eddies  
35 relative to the offshore transport, the offshore current become meander under the  
36 impacts of the anticyclonic mesoscale eddies. The meandered cold tongue and  
37 instability front may stimulate the generation of the small-scale eddies. Unidirectional  
38 uniform wind along cold tongue may also contribute to the formation of the  
39 small-scale eddies.

40

41

## 43 1. Introduction

44        Approximately 90% of the kinetic energy of ocean circulation is contained in  
45 small-scale features, and 50% of the vertical exchange of water mass properties  
46 between the upper and the deep ocean may occur at the submesoscale and mesoscale  
47 (Bouffard et al., 2012). Mesoscale eddies with horizontal scales of 50-500 km can be  
48 observed using altimeters. However, the smaller scale eddies (with horizontal scales  
49 below 50 km) cannot be resolved by conventional altimeters (Liu et al., 2008).  
50 Satellite ocean color sensors provide high-quality observations of the bio-optical  
51 constitute at a spatial resolution better than altimeters. The spatial resolutions of most  
52 ocean color satellites fall in the range of 300 m to 1.1 km (at nadir viewing). The  
53 high-resolution bio-optical observations reveal more details of small-scale  
54 phytoplankton structures. By tracking these small-scale biological features, one can  
55 determine the circulation pattern if the motion speed is large with respect of the  
56 growth and grazing of the phytoplankton (Pegau et al., 2002). Recently, the Medium  
57 Resolution Imaging Spectrometer (MERIS) full-resolution (FR, 300 m) data set is  
58 available publicly. The MERIS FR (300 m) phytoplankton fields are rich in smaller  
59 scale biological features and provide opportunities to study the small-scale processes.  
60 Generally, the time period of the small-scale ocean variability ranges from several  
61 days to several weeks. However, the widely used ocean color data are usually  
62 averaged into weekly or monthly products in order to obtain a large spatial coverage.  
63 This time-averaging may smooth the phytoplankton variability on day-scale (Genin  
64 and Boehlert, 1985). Therefore, the study of the small-scale processes requires higher  
65 space-time resolution of ocean color observation.

66        The South China Sea (SCS) is the largest marginal basin within the western  
67 Pacific, with a total area of 3.5 million km<sup>2</sup> and a basin depth of > 3000 m (0°–25°N,  
68 100°–125°E, figure 1). The SCS is oligotrophic with limited nitrogen and phosphorus  
69 within the euphotic layer. A high abundance of phytoplankton mainly occurs in the  
70 Gulf of Tonkin, the western South China Sea (SCS) and the Sunda Shelf in summer  
71 (Ning et al., 2004). It was reported that a phytoplankton filament in the western SCS  
72 is consistent with the mesoscale eddies transportation and Ekman upwelling (Tang et  
73 al., 2004; Xie et al., 2003; Xiu and Chai, 2011). However, there have been only  
74 limited studies on the small-scale process and its phytoplankton footprints (Nicholson,  
75 2012). In this study, the daily MERIS FR data are used to identify the phytoplankton  
76 variability associated with the small-scale dynamic processes. In this paper, we call  
77 eddies with diameters smaller than 50 km the small-scale eddies, although in some  
78 literatures, they are often called sub-mesoscale eddies (Bassin et al., 2005; Burrage et  
79 al., 2009).

80        The western SCS is one of the dynamically active regions in the SCS (Liu et al.,  
81 2000). A northeastward alongshore current in summer (figure 1) and a southwestward  
82 alongshore current in winter off the east coast of Vietnam are in accordance with wind  
83 stress (Hwang and Chen, 2000; Morimoto et al., 2000; Yuan et al., 2005). The  
84 northeastward alongshore current meanders off the southeastern coast of Vietnam and



85 leaves the Vietnam coast forming an eastward current driven by the southwest wind  
86 paralleled to the coast of eastern Vietnam (Hwang and Chen, 2000; Kuo et al., 2000;  
87 Barthel et al., 2009). The southwesterly monsoon and Ekman transport drive seasonal  
88 upwelling off southeastern Vietnam coast in summer, leading to more than 1°C drop  
89 in sea surface temperature (SST) (Wyrski, 1961; Kuo et al., 2000; Metzger, 2003;  
90 Tang et al., 2006). A cold SST tongue around 12°N extends eastward. The orographic  
91 effect of coastal mountain ridge in the Vietnam can further intensify the southwesterly  
92 wind, and thus significantly enhances the coastal upwelling (Xie et al., 2003; Xie et  
93 al., 2007). The local orographic wind forces the coastal jet separation. This  
94 deformation and movement of coastal water induce mesoscale eddy activities (Gan et  
95 al., 2006; Wang et al., 2008; Chen et al., 2010). An eddy pair in the western SCS  
96 during upwelling season are generated probably due to the vorticity transports from  
97 the nonlinear effect of the western boundary currents (Xie et al., 2003; Ning et al.,  
98 2004; Wang et al., 2006; Chen et al., 2010). Moreover, a pair of anticyclonic eddies  
99 (A-A eddies pairs) in the western SCS during the upwelling season is mentioned by  
100 Kuo et al. (2000) and Xie et al. (2003).

101

## 102 2. Data

103 The study area locates in the western SCS, covering from 5°N-18°N,  
104 105°E-115°E (figure 1). The daily MERIS FR chlorophyll data from 2004 to 2009 are  
105 obtained from the European Space Agency (ESA). The daily 1 km  
106 Moderate-resolution Imaging Spectroradiometer (MODIS) SST data are obtained  
107 from National Aeronautics and Space Administration (NASA) Ocean Color project.

108 The mean sea level anomaly (MSLA) and geostrophic velocity data used here are  
109 extracted from the Delayed-Time Reference Series provided by Archiving, Validation  
110 and Interpretation of Satellite Data in Oceanography (AVISO). The mesoscale eddies  
111 are identified by a new SSH-based (sea surface height) method developed by Chelton  
112 et al. (2011). Rotational speed is computed by

$$113 \quad U = gf^{-1}A/L_s$$

114 Where  $g$  is the gravitational acceleration,  $f$  is the Coriolis parameter,  $A$  is the  
115 eddy amplitude (in centimetres) and  $L_s$  is the eddy length scale (in kilometres),  
116 defined by the radius of the circle that has the same area as the region within the  
117 closed contour of MSLA with maximum average geostrophic current speed (Chelton  
118 *et al.*, 2011).

119 The wind stress is obtained from the [National Oceanic and Atmospheric](#)  
120 [Administration \(NOAA\)](#) Environmental Research Division's Data Access Program  
121 (ERDDAP). The offshore transport ( $M_x$ ) is calculated from

$$122 \quad M_x = \tau_y / f$$

123 Where  $\tau_y$  is the wind stress parallel to the coastline, [positive northward](#). ~~which~~  
124 ~~It is replaced by~~ [with](#) the meridional direction wind stress since the most significant



125 offshore transport ~~in the perpendicular direction~~ to the Vietnam coast is approximately  
126 in the zonal direction.

### 127 **3. Results and discussion**

128 A series of small cyclonic phytoplankton tendrils at the southern edge of the  
129 phytoplankton filament are found during June and October each year over 2004-2009  
130 (figure 2). The phytoplankton tendrils have a mean diameter of 25 km and obviously  
131 rotate out of the filament as the concentration variability of the phytoplankton tendril  
132 seems consistent with the phytoplankton filament concentration variability. It is  
133 implied that the phytoplankton tendril is rotated by the small-scale cyclonic eddy.  
134 High levels of phytoplankton are frequently observed in the center of the small-scale  
135 cyclonic eddies. The reason for this phenomenon will be discussed in the next section.

136 Figure 3 shows an evolution of two cyclonic phytoplankton tendrils during 9 July  
137 2008 and 13 July 2008. It seems that these phytoplankton tendrils have a time scale of  
138 several days. The phytoplankton tendril “A” is less obvious on 9 July 2008. Three  
139 days later, the concentration of phytoplankton tendril “A” increases about  $0.1 \text{ mg m}^{-3}$ .  
140 This high level of phytoplankton mainly occurs at the edge. The phytoplankton levels  
141 in the center are relative low (approximately  $0.07 \text{ mg m}^{-3}$ ). Only one day later, the  
142 phytoplankton concentration in the center increases to approximately  $0.3 \text{ mg m}^{-3}$  and  
143 becomes greater than the level of phytoplankton at the periphery. Another feature is  
144 that the cyclonic “A” tends to propagate eastward. It propagates approximately  $0.1^\circ$   
145 ( $\sim 10 \text{ km}$ ) from 12 July 2008 to 13 July 2008. The western boundary current has a  
146 speed of about  $12 \text{ cm s}^{-1}$  ( $10.4 \text{ km d}^{-1}$ ) in the western SCS during summer (Cai et al.,  
147 2007), which is consistent with the propagation velocity of the small cyclonic eddy  
148 “A”. Therefore, the eastward propagating cyclonic eddy may be driven by the western  
149 boundary current. The small cyclonic eddy B strengthens on 12 July 2008, with high  
150 levels of phytoplankton within its interior. And then it disappears on 13 July 2008.

151 The observation of more detailed phytoplankton distribution in the tendrils is  
152 attributed to the much finer resolution (300 m). We find that there are relative high  
153 phytoplankton levels in the center of the small cyclonic eddies. One possible  
154 mechanism is that the small cyclonic eddies keep rotating high phytoplankton and  
155 perhaps nutrients, leading to the accumulation of phytoplankton in their center.  
156 Another possible mechanism is that the vertical velocity of these small-scale cyclonic  
157 eddies may drive episodic nutrient pulses to the euphotic zone to stimulate  
158 phytoplankton growth (Lévy et al., 2012). Figure 4 shows the sea surface temperature  
159 distribution associated with the phytoplankton tendril “A”. It is obvious that the cold  
160 water is transported away from the cold tongue by the small-scale eddies. And the low  
161 temperature water firstly occurs in the periphery of the eddies. Different from the  
162 majority of mesoscale cyclonic eddy, there is not significant lower temperature water  
163 in the center. It is implied that there is no upwelling or vertical mixing in the center.  
164 Therefore, the phytoplankton distribution over this small-scale eddy may be  
165 dominated by horizontal movement, and the relative high phytoplankton level in the  
166 center of the cyclonic eddies “A” could be attributed to the accumulation of

167 phytoplankton or nutrients from the outer edge to interior under the rotation effect.

168 The small-scale eddies strengthen the horizontal diffusion of the nutrients and  
169 phytoplankton (Capet et al., 2008a). These small cyclonic eddies are mainly observed  
170 at the front of the filament, where strong differences in water mass properties result in  
171 high strain rates and instabilities. Meanwhile, the small-scale eddies are also  
172 associated with the occurrence of an anticyclonic mesoscale ~~eddies-eddy~~  
173 of the filament (figure 3(a)). However, the small-scale cyclonic eddy does not occur  
174 for the entire period of the offshore Ekman transport and the anticyclonic eddy. It only  
175 arises at certain stages. We analyzed the offshore Ekman transport ( $M_x$ ) and rotation  
176 speed of the anticyclonic eddies during the development of the small-scale eddies  
177 over the period of July 2008 shown in figure 3. Due to the limits of the cloud  
178 coverage and satellite passing time, the image showing the declination of small-scale  
179 eddies is not available. However, it is found that the small-scale eddies disappear on  
180 22 July 2008. Figure 3 (a) and (b) imply that the small-scale eddies may initially form  
181 on 9 July 2008. Therefore, we presumed that the small-scale eddies occur during the  
182 9-22 July. Figure 5 indicates that the offshore transport ( $M_x$ ) decreases first and then  
183 increases rapidly on 16 July. Different from the variability of  $M_x$ , the rotation speed  
184 increases from  $0.33 \text{ m s}^{-1}$  on 2 July to  $0.42 \text{ m s}^{-1}$  on 12 July. And then it starts to  
185 decrease to approximately  $0.4 \text{ m s}^{-1}$  on 16 July. At last, the rotation speed increases  
186 associated with the strengthening of  $M_x$ . The variability of  $M_x$  seems not consistent  
187 with the variability of the levels of phytoplankton (figure 3). The levels of  
188 phytoplankton has a significant increases from 9 July to 13 July, accompanying with  
189 the decreases of the  $M_x$ . This may be due to a lag between nutrients input and  
190 phytoplankton growth. The normalized rotation speed of the anticyclonic eddy is  
191 defined as the ratio of the rotation speed and the  $M_x$ , which indicates the relative  
192 movement between the anticyclonic eddy and the offshore transport. The variability of  
193 the normalized rotation speed shows that the small-scale eddies is associated with the  
194 greater relative movement between the anticyclonic eddy and the offshore transport  
195 (figure 5). The offshore current becomes ~~to~~-meander under the influence of the  
196 anticyclonic eddy when the offshore transport turns weaker and the rotation speed of  
197 the anticyclonic eddy increases. The meandering current may stimulate the generation  
198 of the small-scale process (Capet et al., 2008a, b).

199 The phytoplankton filament is consistent with the cold tongue induced by the  
200 offshore Ekman transport, which is associated with negative sea surface height  
201 anomaly relative to surround light and warm water. The small-scale eddies extend  
202 from the cold tongue along the front. Therefore the heavy and cold water firstly  
203 occurs in the periphery of small-scale eddies. Along the front, the transport from the  
204 surface heavy water to the light water may be forced by the wind. Throughout the  
205 development of the small-scale eddies, the wind direction exhibits some variations  
206 (figure 6). Wind blowing varies from west-southwest (WSW) on 2 July 2008 (before  
207 the generation of the small-scale eddies) to southwest (SW) on 9-13 July 2008 (during  
208 the presence of the small-scale eddies). It implies that the small-scale eddies tends  
209 to be associated with the more unidirectional uniform wind blowing along the  
210 phytoplankton filament. Under spatially uniform wind forcing, the changed

211 meandering current may be more likely to generate the small-scale structure  
212 (McGillicuddy et al., 2007; Mahadevan et al., 2008).

#### 213 **4. Conclusion**

214 This paper describes the small-scale cyclonic eddies in the western SCS. Driven  
215 by the small-scale cyclonic eddies, a series of phytoplankton tendrils occur at the  
216 southern front of the wind-driven offshore current. These small-scale eddies have  
217 horizontal scales less than 50 km and propagate eastward at the speed of  $12 \text{ cm s}^{-1}$ ,  
218 accompanying with offshore current. Offshore current, the mesoscale anticyclonic  
219 eddies and wind field may contribute to the generation of the small-scale cyclonic  
220 eddies. Horizontal transport by the small-scale cyclonic eddies stimulates the  
221 diffusion of the nutrients and phytoplankton of the western SCS.

#### 222 **Acknowledgements**

223 We gratefully thank Ruixin Huang and Ian Jones for helpful comments and  
224 suggestions. The MERIS 300 m chlorophyll data was provided by ESA-MOST  
225 Dragon 3 Cooperation Programme from the European Space Agency. The sea surface  
226 height and geostrophic current data were obtained from the Archiving Validation and  
227 Interpretation of Satellite Data in Oceanography (AVISO). The MODIS sea surface  
228 temperature was obtained from the NASA ocean color project. The wind stress is  
229 obtained from the [National Oceanic and Atmospheric Administration \(NOAA\)](#)  
230 Environmental Research Division's Data Access Program (ERDDAP). The research  
231 was supported by the "Strategic Priority Research Program" of the Chinese Academy  
232 of Sciences (No. XDA11010302), the Public science and technology research funds  
233 projects of ocean (No. 201205040-6), the Innovation Group Program of State Key  
234 Laboratory of Tropical Oceanography, South China Sea Institute of Oceanology,  
235 Chinese Academy of Sciences (No. LTOZZ1201) and the National Natural Science  
236 Foundation of China (No. 41006111).

#### 237 **References**

- 238 Barthel, K., Rosland, R., and Thai, N.C.: Modelling the circulation on the continental  
239 shelf of the province Khanh Hoa in Vietnam, *J. Marine Syst.*, 77(1-2), 89-113, 2009.
- 240 Bassion, C.J., Washburn, L., Brzezinski, M., and McPhee-Shaw, E.: Sub-mesoscale  
241 coastal eddies observed by high frequency radar: A new mechanism for delivering  
242 nutrients to kelp forests in the Southern California Bight, *Geophys. Res. Lett.*, 32,  
243 L12604, 2005.
- 244 Bouffard, J., Renault, L., Ruiz, S., Pascual, A., Dufau, C., and Tintoré, J.: Sub-surface  
245 small-scale eddy dynamics from multi-sensor observations and modeling, *Progr.*  
246 *Oceanogr.*, 106, 62-79, 2012.
- 247 Burrage, D.M., Book, J.W., Martin, P.J.: Eddies and filaments of the Western Adriatic  
248 Current near Cape Gargano: Analysis and prediction, *J. Marine Syst.*, 78, S205-S226,  
249 2009.
- 250 Cai, S., Long, X., and Wang, S.: A model study of the summer Southeast Vietnam  
251 Offshore Current in the southern South China Sea, *Cont. Shelf Res.*, 27, 2357-2372,

252 2007.

253 Capet, X., McWilliams, J.C., Molemaker, M.J., and Shchepetkin, A.F.: Mesoscale to  
254 submesoscale transition in the California Current System. Part I: Flow structure, eddy  
255 flux, and observational tests, *J. Phys. Oceanogr.*, 38, 29–43, 2008a.

256 Capet, X., McWilliams, J.C., Molemaker, M.J., and Shchepetkin, A.F.: Mesoscale to  
257 submesoscale transition in the California Current System, Part II: Frontal processes. *J.*  
258 *Phys. Oceanogr.*, 38, 44–64, 2008b.

259 Chelton, D.B., Schlax, M.G., and Samelson, R.M.: Global observations of nonlinear  
260 mesoscale eddies, *Prog. Oceanogr.*, 91(2), 167-216, 2011.

261 Chen, G., Hou, Y., Zhang, Q., and Chu, X.: The eddy pair off eastern Vietnam:  
262 Interannual variability and impact on thermohaline structure, *Cont. Shelf Res.*, 30(7),  
263 715-723, 2010.

264 Gan, J., Li, H., Curchitser, E.N., and Haidvogel, D.B.: Modeling South China Sea  
265 circulation: Response to seasonal forcing regimes, *J. Geophys. Res.*, 111(C6), C06034,  
266 2006.

267 Genin, A., and Boehlert, G.W.: Dynamics of temperature and chlorophyll structures  
268 above a seamount: An oceanic experiment, *J. Marine Syst.*, 43(4), 907-924, 1985.

269 Huang, B., Hu, J., Xu, H., Cao, Z., and Wang D.: Phytoplankton community at warm  
270 eddies in the northern South China Sea in winter 2003/2004, *Deep-Sea Res. Pt. II*, 57,  
271 1792-1798, 2010.

272 Hwang, C., and Chen S.-A.: Circulations and eddies over the South China Sea derived  
273 from TOPEX/Poseidon altimetry, *J. Geophys. Res.*, 105(C10), 23943-23965, 2000.

274 Kuo, N.-J., Zheng, Q., and Ho, C.-R.: Satellite Observation of Upwelling along the  
275 Western Coast of the South China Sea, *Remote Sens. Environ.*, 74(3), 463-470, 2000.

276 Lévy, M., Ferrari, R., Franks, P.J.S., Martin, A.P., and Rivière, P.: Bringing physics to  
277 life at the submesoscale, *Geophys. Res. Lett.*, 39, L14602, 2012.

278 Liu, Y., Weisberg, R.H., and Yuan, Y.: Patterns of upper layer circulation variability  
279 in the South China Sea from satellite altimetry using the Self-Organizing Map, *Acta*  
280 *Oceanol. Sin.*, 27(Supp.), 129-144, 2008.

281 Liu, Y., Yuan, Y., Su, J., and Jiang, J.: Circulation in the South China Sea in summer  
282 of 1998, *Chinese Sci. Bull.*, 45(18), 1648-1655, 2000.

283 Mahadevan, A., Thomas, L.N., and Tandon, A.: Comment on "eddy/wind interactions  
284 stimulate extraordinary mid-ocean plankton blooms", *Science*, 320, 448, 2008.

285 McGillicuddy, D.J., Anderson, L.A., Bates, N.R., Bibby, T., Buesseler, K.O., Carlson,  
286 C.A., Davis, C.S., Ewart, C., Falkowski, P.G., Goldthwait, S.A., Hansell, D.A.,  
287 Jenkins, W.J., Johnson, R., Kosnyrev, V.K., Ledwell, J.R., Li, Q.P., Siegel, D.A., and  
288 Steinberg, D.K.: Eddy/wind interactions stimulate extraordinary mid-ocean plankton  
289 blooms, *Science*, 316, 1021-1026, 2007.

290 Metzger, E.: Upper Ocean Sensitivity to Wind Forcing in the South China Sea, *J.*  
291 *Oceanogr.*, 59(6), 783-798, 2003.

292 Morimoto, A., Yoshimoto, K., and Yanagi, T.: Characteristics of sea surface  
293 circulation and eddy field in the South China Sea revealed by satellite altimetric data,  
294 *J. Oceanogr.*, 3, 331-344, 2000.

295 Nicholson, S.: Linking small-scale circulation dynamics with large-scale seasonal

296 production (phytoplankton) in the Southern Ocean, 4th CSIR Biennial Conference:  
297 Real problems relevant solutions, CSIR, Pretoria, 9-10 October 2012  
298 Ning, X., Chai, F., Xue, H., Cai, Y., Liu, C., and Shi, J.: Physical-biological  
299 oceanographic coupling influencing phytoplankton and primary production in the  
300 South China Sea, *J. Geophys. Res.*, 109(C10), C10005, 2004.  
301 Pegau, W., Boss, E., and Martínez, A.: Ocean color observations of eddies during the  
302 summer in the Gulf of California, *Geophys. Res. Lett.*, 29(9), 1-3, 2002.  
303 Tang, D.L., Kawamura, H., Shi, P., Takahashi, W., Guan, L., Shimada, T., Sakaida, F.,  
304 and Isoguchi, O.: Seasonal phytoplankton blooms associated with monsoonal  
305 influences and coastal environments in the sea areas either side of the Indochina  
306 Peninsula, *J. Geophys. Res.*, 111(G1), G01010, 2006.  
307 Tang, D., Kawamura, H., Dien, T., and Lee, M.: Offshore phytoplankton biomass  
308 increase and its oceanographic causes in the South China Sea, *Mar. Ecol. Prog. Ser.*  
309 268, 31-41, 2004.  
310 Wang, G., Chen, D., and Su, J.: Generation and life cycle of the dipole in the South  
311 China Sea summer circulation, *J. Geophys. Res.*, 111(C6), C06002, 2006.  
312 Wang, G., Chen, D., and Su, J.: Winter Eddy Genesis in the Eastern South China Sea  
313 due to Orographic Wind Jets, *J. Phy. Oceanogr.*, 38(3), 726-732, 2008.  
314 Wyrтки, K.: *Physical Oceanography of the Southeast Asian waters*, NAGA Rep. 2,  
315 195 pp., Scripps Inst. Oceanogr, La Jolla, Calif, 1961.  
316 Xie, S.-P., Xie, Q., Wang, D., and Liu, W.T.: Summer upwelling in the South China  
317 Sea and its role in regional climate variations, *J. Geophys. Res.*, 108(C8), 3261, 2003.  
318 Xie, S.-P., Chang, C.-H., Xie, Q., and Wang D.: Intraseasonal variability in the  
319 summer South China Sea: Wind jet, cold filament, and recirculations, *J. Geophys.*  
320 *Res.*, 112(C10), C10008, 2007.  
321 Xiu, P., and Chai, F.: Modeled biogeochemical responses to mesoscale eddies in the  
322 South China Sea, *J. Geophys. Res.*, 116(C10), C10006, 2011.  
323 Yuan, Y., Liu, Y., Liao, G., Lou, R., Su, J., and Wang, K.: Calculation of circulation in  
324 the South China Sea during summer of 2000 by the modified inverse method, *Acta*  
325 *Oceanol. Sin.*, 24(1), 14-30, 2005.

326 Figure captions

327 Figure 1. (a) Bathymetry of the South China Sea (Unit: m), the red rectangle  
328 represents the study area. (b) Mean surface geostrophic currents in June-October of  
329 2002-2008.

330

331 Figure 2. Daily 300 m MERIS chlorophyll (unit:  $\text{mg m}^{-3}$ ) on (a)-(b) 5 September 2004,  
332 (c)-(d) 22 June 2005, (e)-(f) 7 June 2006, (g)-(h) 21 July 2007, (i)-(j) 16 July 2008,  
333 (k)-(l) 29 July 2009. The cloud covered area is masked by the white color.

334

335 Figure 3. Daily 300 m MERIS chlorophyll (unit:  $\text{mg m}^{-3}$ ) on (a) 9 July 2008, (b) 12  
336 July 2008, (c) 13 July 2008. The cloud covered area is masked by the white color. 'A'  
337 and 'B' indicate two small cyclonic eddies respectively. The pink circle in (a) denotes  
338 the anticyclonic mesoscale eddy (AME) on 9 July 2008, which is derived from  
339 AVISO MSLA data following the method of Chelton et al. (2011).

340

341 Figure 4. MODIS 1 km sea surface temperature distribution (unit:  $^{\circ}\text{C}$ ) on 13 July  
342 2008.

343

344

345 Figure 5. The offshore transport ( $M_x$ ,  $\text{kg m}^{-1} \text{s}^{-1}$ ), rotation speed of the mesoscale  
346 anticyclonic eddy ( $U$ ,  $\text{cm s}^{-1}$ ) and the normalized rotation speed to  $M_x$  ( $U/M_x$ ),  
347 indicating the relative importance of the mesoscale anticyclonic eddy and offshore  
348 Ekman transport in the form of small-scale eddies.

349

350 Figure 6. Wind field on 2 July 2008 (the blue arrow), 12 July 2008 (the red arrow) and  
351 26 July 2008 (the green arrow).

352

353

354

355

356

357

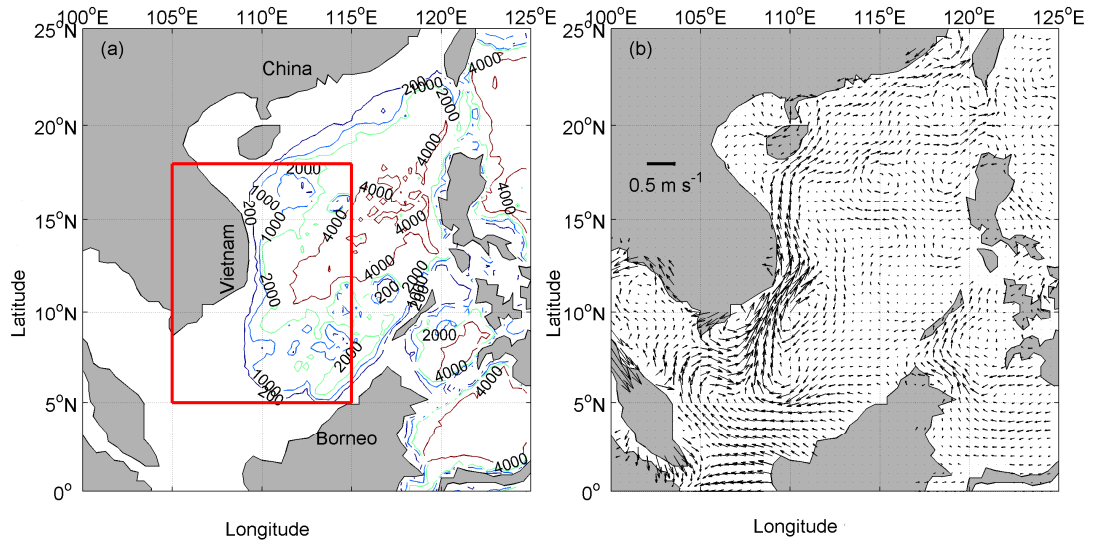
358

359



360 Figures

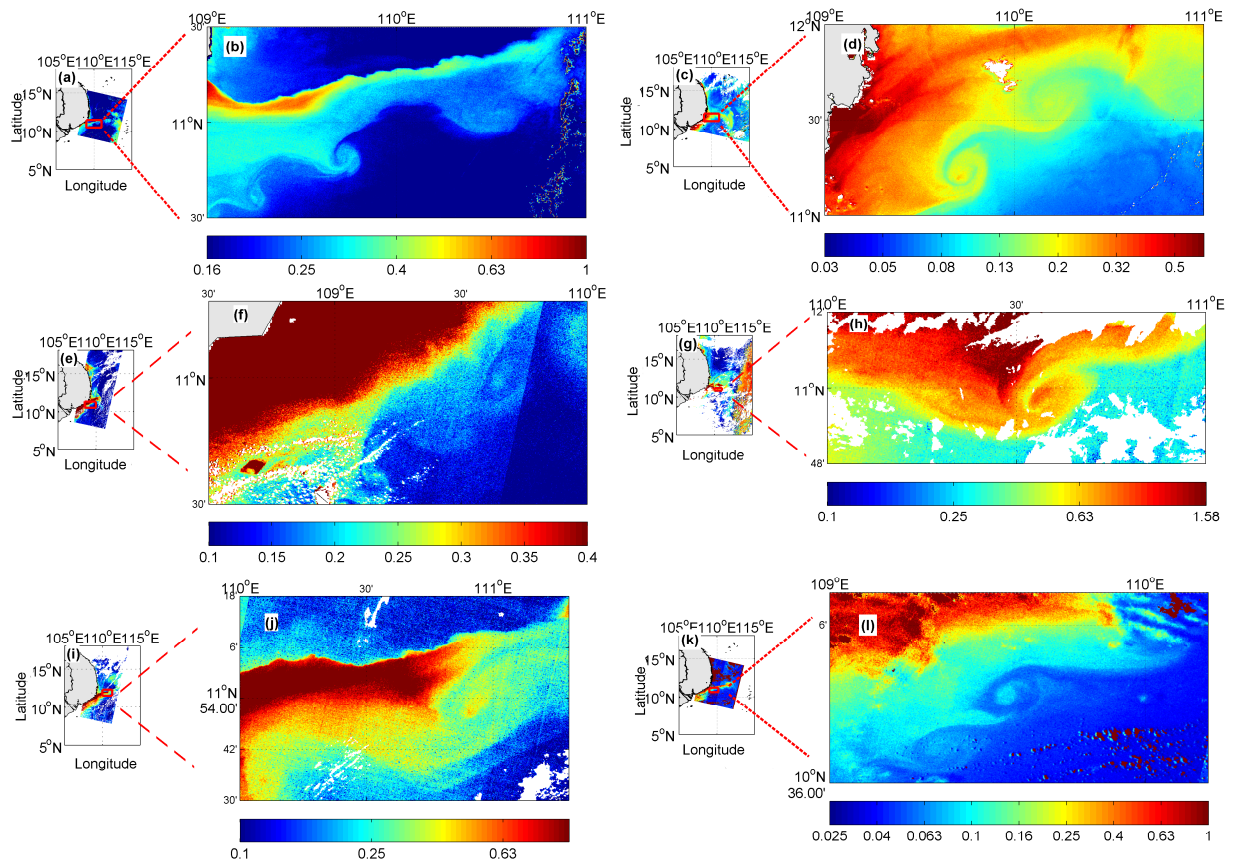
361 Figure 1



362

363

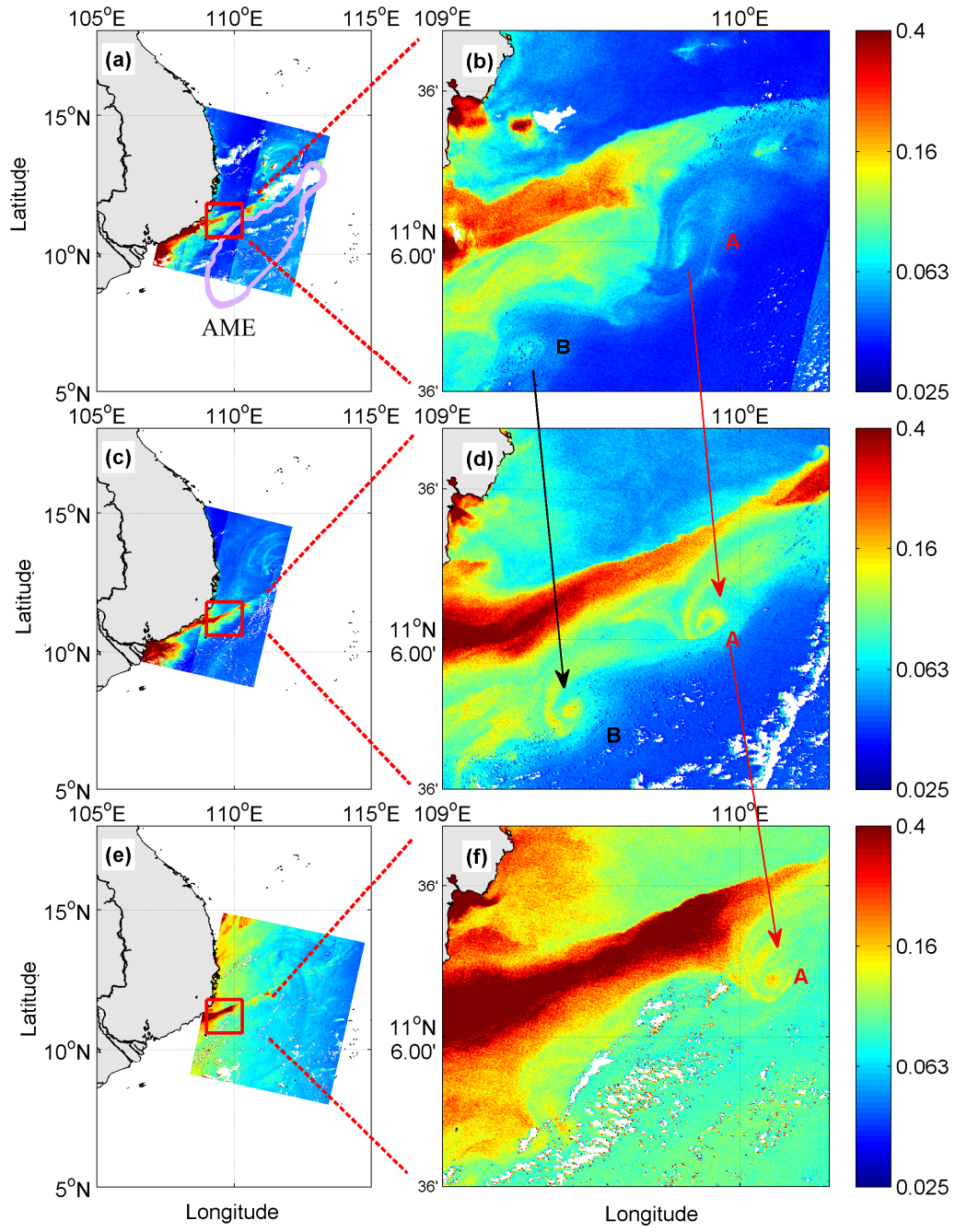
364 Figure 2



365



366 Figure 3



367

368

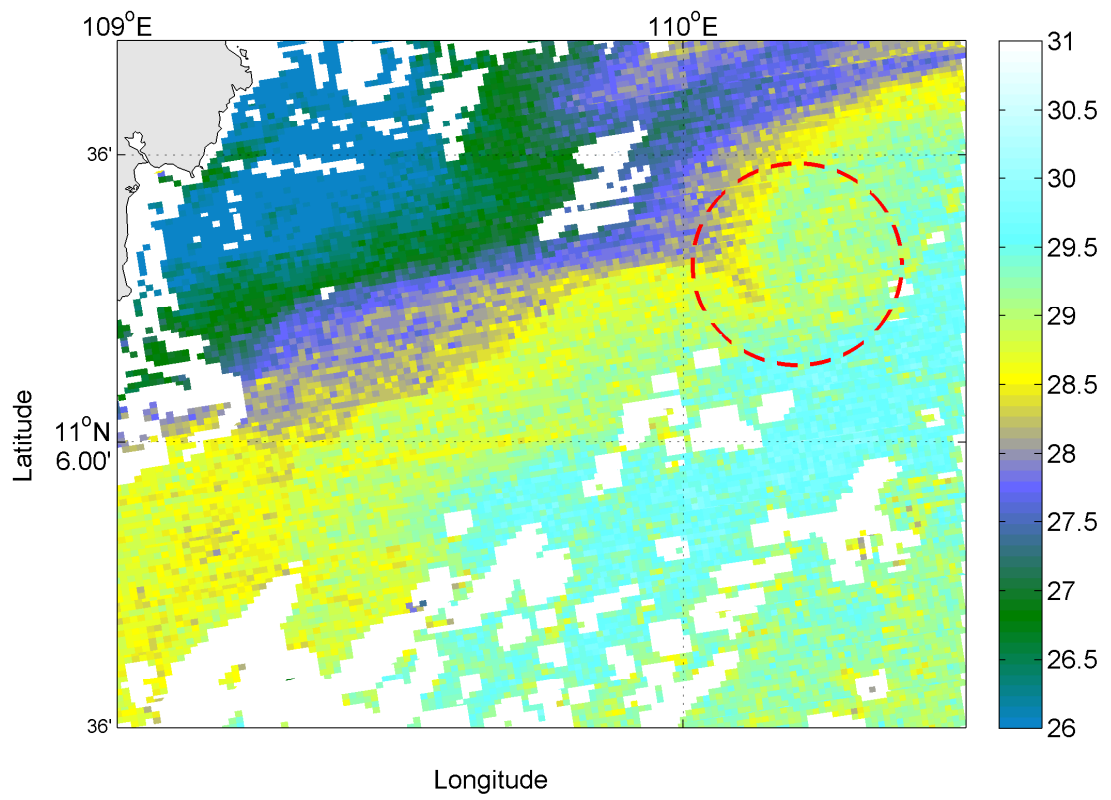
369

370

371

372

373 Figure 4



374

375

376

377

378

379

380

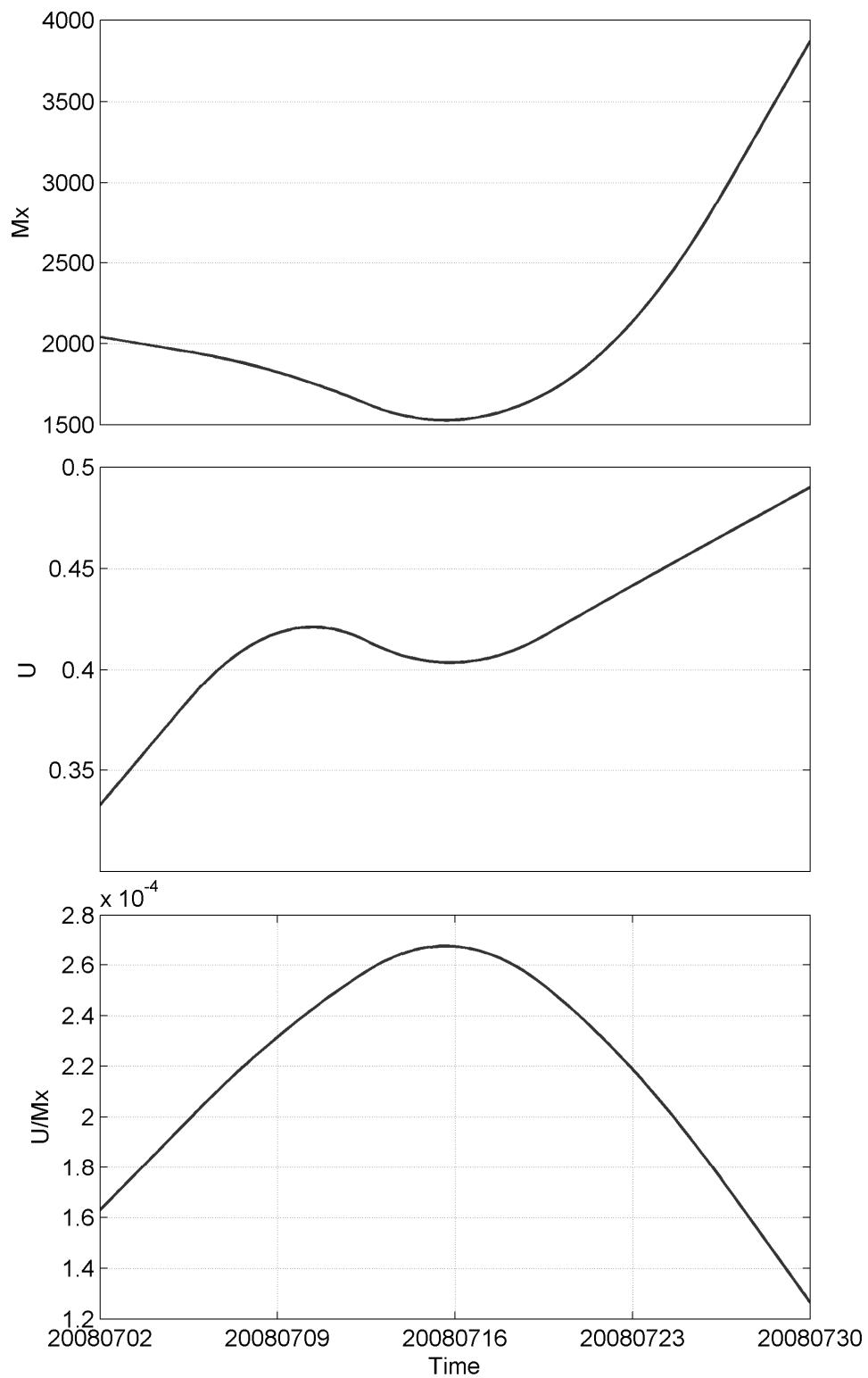
381

382

383

384

385 Figure 5

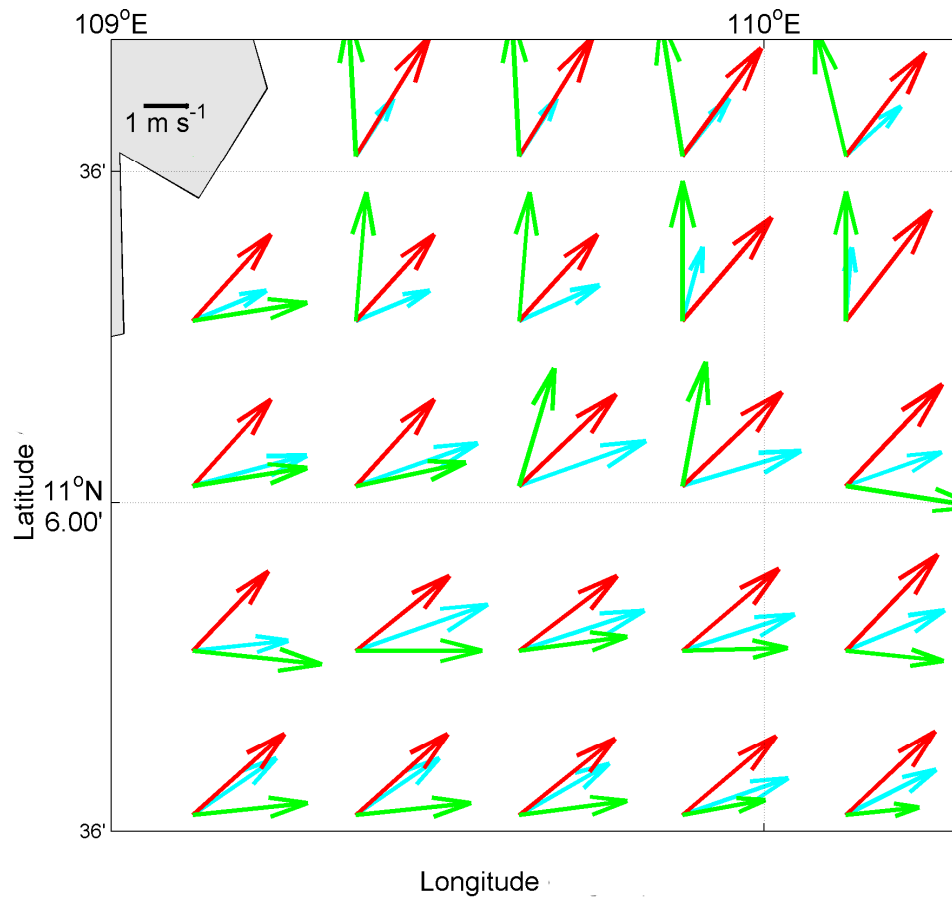


386

387

388

389 Figure 6



390